Anion/Naphthalenediimide Interactions in a Pd(II)-Based Tetrameric Metallocycle

Monica A. Gordillo, Paola A. Benavides, and Sourav Saha*

Department of Chemistry, Clemson University, Clemson, South Carolina 29634, United States

*Email: souravs@clemson.edu

ABSTRACT

A tetrameric metallocycle [Pd(dppp)(DPNDI)]4·8TfO consisting of four dppp-capped Pd(II) corners (dppp = 1,3-bis(diphenylphosphonium)ethane) and four linear π -acidic N,N'-di(4-pyridyl)-1,4,5,8-naphthalene diimine (DPNDI) ligands has been synthesized and its single crystal structure has been elucidated for the first time. The crystal structure of the metallocycle revealed anion- π , lone-pair- π , and CH···anion interactions between electron deficient DPNDI ligands and TfO⁻ counterions and provided valuable insights into its anion recognition and metathesis capabilities. The ¹H, ¹⁹F, ³¹P and NMR studies demonstrated that in noncoordinating solvents, such as nitromethane and dichloromethane, [Pd(dppp)(DPNDI)]8+ metallocycle underwent anion exchange in a single-crystal to single-crystal fashion without any structural changes. However, the metallocycle experienced slow dissociation in a polar solvent DMSO, which could be reversed easily by thermal treatment.

Owing to well-defined coordination geometries of transition metal ions and organic ligands and selfrectifying dynamic nature of metal-ligand coordination bonds, metallocycles, 1-3 metallocages, 4-6 and metal-organic frameworks^{4,8} have emerged as attractive platforms for myriad guest recognition, separation, and delivery-related applications. Unlike covalent organic macrocycles, which face significant enthalpic and entropic costs stemming from conformational changes of acyclic precursors and diminished degrees of freedom during synthesis and rely heavily on the templating effect to overcome these barriers, 9-11 metallocycles and cages benefit from the delicate balance between the enthalpic gain stemming from metalligand coordination, the reversibility of coordination bonds that makes such macrocyclization a selfrectifying process controllable under kinetic or thermodynamic conditions, and the precise geometries and topologies of metal ions and organic ligands that provide *in-situ* preorganization even in the absence of third-party templating agents. Pioneering work by Stang, ¹² Fujita, ¹³ and number of other researchers ^{14–17} have shown that reactions between cis-capped square-planar Pd(II) and Pt(II) complexes and linear 4,4'bipyridine (BPY) and extended bipyridyl ligands not only lead to macrocyclization over polymerization, but more importantly, the shapes of the resulting metallocycles (triangles vs. squares) can be controlled by regulating precursor concentrations, solvent polarity, and reaction temperatures. ^{18,19} Although the relatively short, rigid BPY ligand often yielded crystalline metallocycles suitable for single crystal structure elucidation, 18,20 the π -extended and functionally more active ligands containing pyrene, 21 pervlene 19 and perylenediimide¹⁴ cores afforded metallocycles and cages that were only characterized thus far by circumstantial evidences obtained from NMR and mass spectrometric analyses. The lack of direct crystallographic evidence, however, made it difficult to identify weak host-guest interactions, such as anion $-\pi$, 22 lone-pair $-\pi$, 23 and CH···anion 24 interactions, which do not necessarily engender meaningful spectroscopic or electrochemical changes in the receptors. For example, while the crystal structures of dipyridyl-tetrazine based metallo-squares and pentagons revealed the existence of anion- π interactions and the templating effects of tetrahedral and octahedral charge diffuse anions, ^{25,26} the lack of crystal structures of dipyridyl-perylenediimide-based metallocycles¹⁴ left us in the dark about their anion recognition capabilities. Extensive studies in our laboratory^{27–30} and elsewhere^{31,32} over the past decade have revealed that in aprotic mediums, π -acidic 1,4,5,8-naphthalenediimide (NDI) compounds can discriminate anions on the basis of their electron donating capability, which is accurately reflected from their Lewis basicity: Depending on their π -acidity, NDI compounds undergo (i) ground-state or thermal electron transfer from highly Lewis basic anions, such as OH-, F-, and CN- and photoinduced electron transfer from less Lewis basic anions such as Cl⁻ and AcO⁻, generating paramagnetic NDI⁻ radical anions, ²⁹ (ii) form diamagnetic charge-transfer complexes with non-basic anions such as Br⁻ and $I_{\tau}^{-,29}$ and (iii) form anion- π complexes with multinuclear charge-diffuse anions, such as TfO⁻ and ClO₄^{-.33-35} Although π -donor/acceptor host-guest interaction has been characterized by X-ray crystallography in a DPNDI-based metallocycle, 36 to our

knowledge, there is no crystallographic evidence of anion/NDI interaction in NDI-based metallocycles. The crystal structure of a $[Pd(dppe)(DPNDI)]_n^{2n+}$ (dppe = 1,3-bis(diphenylphosphonium)ethane, DPNDI = N,N'-di(4-pyridyl)NDI) coordination polymer³³ synthesized earlier in our laboratory presented the first concrete evidence of anion– π interaction between TfO⁻ anions and DPNDI ligands, however, the dppe-capped Pd(II) corners failed to yield a metallocyclic receptor possibly because of large bite-angle of the capping ligands. By introducing a dppp-capped (dppp = 1,2-bis(diphenylphosphonium)propane) square-planar Pd(II) corner, herein, we synthesized a DPNDI-based tetrameric metallosupramolecular rhombus (Scheme 1), elucidated its crystal structure for the first time, and demonstrated its anion recognition and anion exchange capabilities based on X-ray crystallography, 1 H, 19 F, and 31 P NMR spectroscopies, and electrochemistry.

Scheme 1. The self-assembly of a novel [Pd(dppp)(DPNDI)]4.8TfO metallacycle.

A room temperature reaction between Pd(dppp)·2TfO complex and DPNDI ligand (60 μ mol each) in MeNO₂ (10 mL) for 48 h, followed by slow Et₂O vapor diffusion into the reaction mixture yielded pale yellow crystals of tetrametic [Pd(dppp)(DPNDI)]₄·8TfO metallocycle (Figure 1) suitable for single-crystal X-ray diffraction (SXRD) analysis. The SXRD data revealed the structure of a rhombus-shaped metallocycle consisting of four dppp-capped Pd(II) corners linked by four linear DPNDI ligands. The \angle Pd-Pd angles in this rhombohedral metallocycle were ca. 80° and 100° and the Pd-Pd distances along the sides were 19.5 Å. The NDI-cores of two opposite arms were almost coplanar with the mean metallocycle plane defined by four coplanar Pd(II) corners, while the other two NDI cores deviated slightly from the mean plane. The octacationic metallacycle was accompanied by eight TfO⁻ anions involved in anion- π , lone-pair- π , and CH···anion interactions with the DPNDI ligands. The short contacts between the O-atoms of TfO⁻ anions and the carbonyl-C as well as the center of the electron deficient imide rings of DPNDI ligands ($d_{O-C} = 2.93-3.11$ Å < the sum of corresponding van der Waals radii of ~3.22 Å) provided clear indications of anion- π interactions. Furthermore, one of the F-atoms of certain TfO⁻ anions also remained in close contact (centroid distance ~2.57 Å, which is ca. 0.6 Å shorter than the sum of van der Waals radii) with the electron deficient aromatic core of DPNDI, while another F-atom formed a H-bond ($d_{F-H} = 2.46$

Å) with the H-atom *ortho*- to the pyridyl-N. These distinct but relatively weak supramolecular interactions rendered [Pd(dppp)(DPNDI)]₄⁸⁺ metallocycle an attractive anion recognition and exchange platform, which we investigated through NMR experiments.

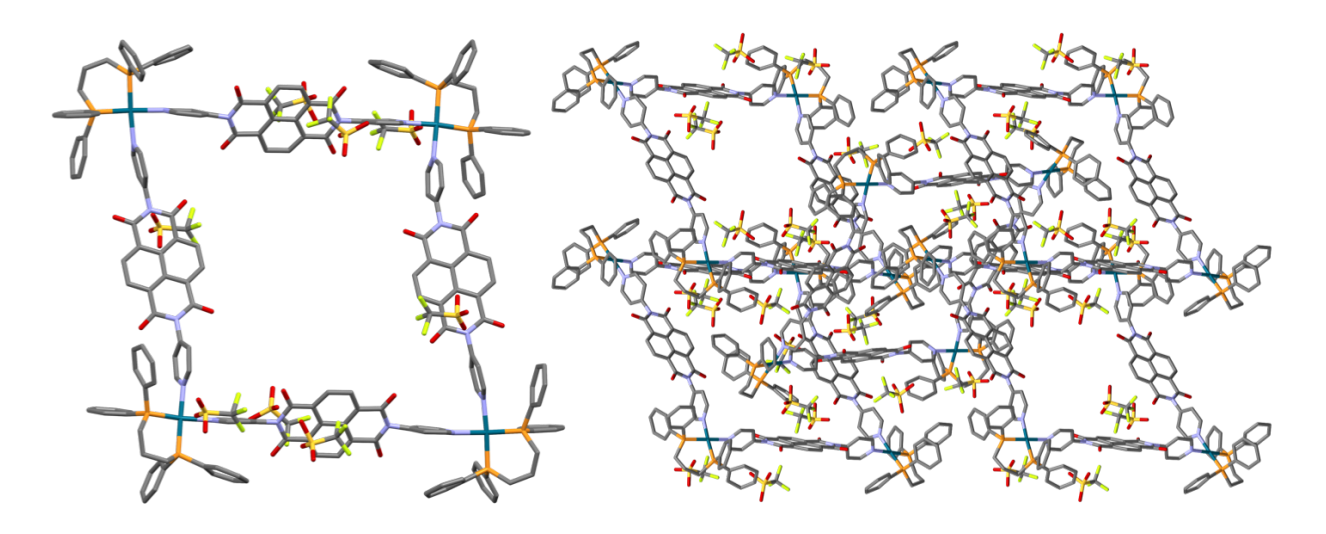


Figure 1. The single crystal structure of [Pd(dppp)(DPNDI)]₄·8TfO metallacycle showing various modes of anion/DPNDI interactions (left) and how the metallocycles are packed (right).

Furthermore, the progress of [Pd(dppp)(DPNDI)]₄·8TfO metallocycle formation was also monitored by ¹H and ³¹P NMR spectroscopies. Soon after mixing stoichiometric amounts of Pd(dppp)(OTf)₂ corner and DPNDI ligand in CD₃NO₂, the characteristic ¹H NMR signals of the metallosupramolecular rhombus appeared as dominant peaks along with few very low intensity peaks corresponding to other unidentified species (Figure 2a). These peaks and their relative intensities remained practically unchanged over time, suggesting that in CD₃NO₂, the metallocycle formation was favored, and once formed, it did not equilibrate or dissociate into other species. Consistent with these observations, ³¹P NMR studies (Figure 2b) also showed one dominant peak at ~8 ppm corresponding to the metallocycle and a very faint signal (~8.8 ppm) indicative of another minor species. Both new peaks were distinct from the characteristic signal of Pd(dppp)(OTf)₂ corner (~20 ppm), confirming that the Pd(dppp)(OTf)₂ precursor was fully consumed. Like ¹H NMR, ³¹P NMR signals also did not change over time, verifying slow (or the lack of) equilibrium between the preferred macrocycle and other minor species. Nevertheless, only tetrameric [Pd(dppp)(DPNDI)]₄·8TfO metallocycle precipitated out during crystallization and the isolated pure material was used for further studies.

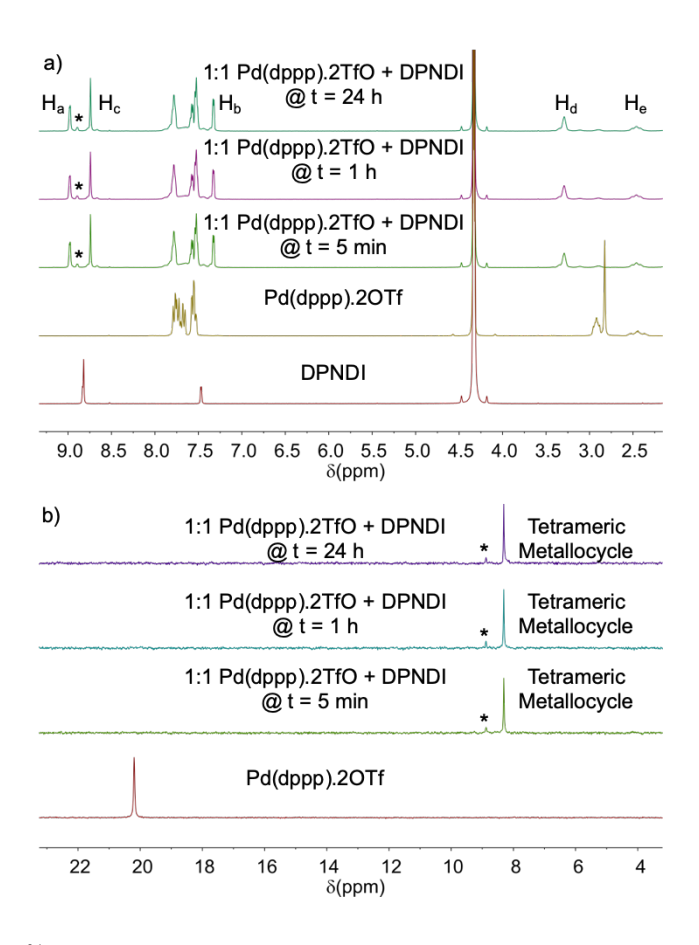


Figure 2. The 1 H (a) and 31 P (b) NMR spectra of 1:1 mixture of Pd(dppp)(OTf)₂ and DPNDI in CD₃NO₂ recorded over time (t = 5 min to 24 h) demonstrating a fairly rapid formation of tetrameric [Pd(dppp)(DPNDI)]₄·8TfO metallacycle as the predominant product and a very small amount of an unidentified species indicated by the *-labeled peaks.

Having determined the formation and structure of [Pd(dppp)(DPNDI)]₄·8TfO metallacycle and how the TfO⁻ counterions and DPNDI ligands were involved in multimodal supramolecular interactions, we turned our attention to investigate its anion exchange behavior through 1 H and 19 F NMR spectroscopies. Anion metathesis was performed on pre-synthesized and isolated solid [Pd(dppp)(DPNDI)]₄·8TfO by suspending it in 1 M Bu₄NX/CH₂Cl₂ solutions, as well as *in-situ* by adding 1 M Bu₄NX/MeNO₂ solutions into the reaction mixture after allowing the formation of metallocycle. Upon addition of Bu₄N⁺X⁻/MeNO₂ solutions to *in-situ* prepared metallocycle solutions, the octacationic metallocycle containing mostly the exchanged counterion precipitated out, which was washed thoroughly and dried before the NMR studies. Irrespective of the counterions (X⁻ = TfO⁻, ReO₄⁻, PF₆⁻, and BF₄⁻), the freshly prepared solutions of pristine and anion-exchanged (solid-state and *in-situ*) [Pd(dppp)(DPNDI)]₄⁸⁺ metallocycle displayed characteristic 1 H NMR signals (Figure 2) of the NDI-core (singlet, ca. 8.7 ppm) and pyridyl rings (2 doublets, ca. 8.8 and 7.7 ppm) of DPNDI linkers and the phenyl rings (multiplet, ~7.5 ppm) and propylene chain (2.9 (m) and

1.9 (m) ppm) of dppp ligands. Interestingly, the core NDI proton signal appeared at slightly more upfield positions (\sim 8.72 ppm) in the presence of TfO⁻ and PF₆⁻ anions than with ReO₄⁻ and BF₄⁻ anions (\sim 8.74 ppm), suggesting that the former enjoyed marginally stronger anion/NDI interactions and exerted commensurately greater shielding effect on the π -acidic DPNDI ligands. The more downfield location of H_a signal (*ortho* to the pyridyl-N) in the presence of CF₃SO₃⁻ counterion could be attributed to H···F H-bonding interaction between the anion and that proton, which was evident from the crystal structure. Such interaction was likely absent in the presence of other counterions, causing the H_a signal to appear at more upfield positions. Like ¹H NMR signals, the characteristic ³¹P NMR spectra of [Pd(dppp)(DPNDI)]₄⁸⁺ metallocycle also remained unchanged and showed only one peak for the dppp ligand after solid-state exchange of the original TfO⁻ counterions with ReO₄⁻ and PF₆⁻ (Figure 3b), confirming that the metallocycle remained intact upon anion metathesis. The presence of PF₆⁻ anion after the exchange was observed.

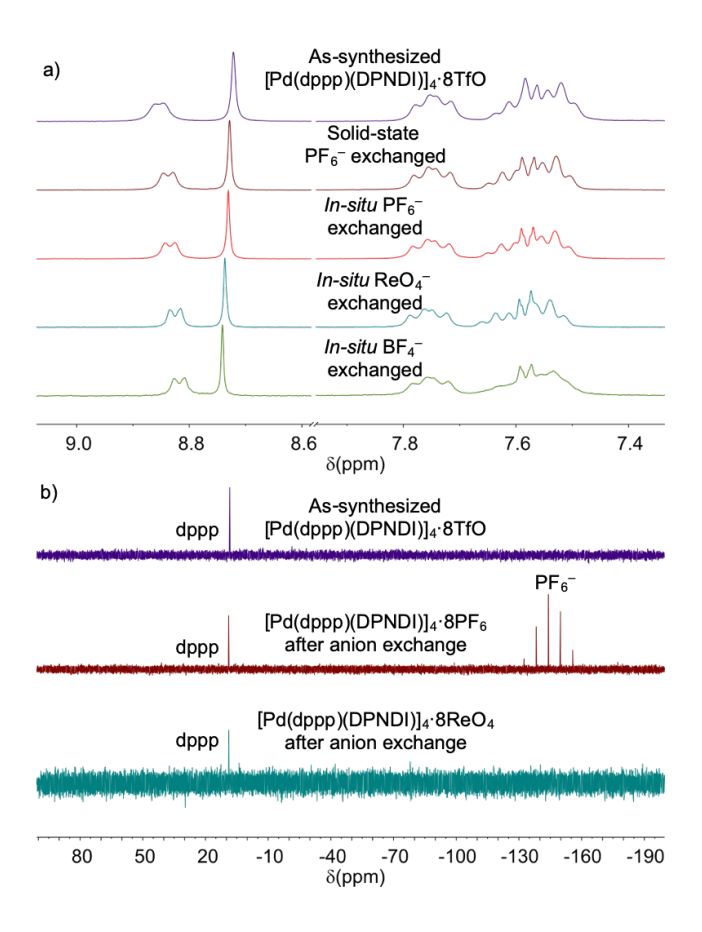


Figure 3. (a) The ¹H and (b) ³¹P NMR spectra of [Pd(dppp)(DPNDI)]₄⁸⁺ metallocycle before and after anion exchange demonstrating that the metallocycle remained intact after replacing original TfO⁻ anion with other charge diffuse anions.

The anion exchange phenomenon was further verified by ¹⁹F NMR spectroscopy (Figure 3), which revealed a characteristic CF₃SO₃⁻ peak (–77.74 ppm) in freshly prepared [Pd(dppp)(DPNDI)]₄·8TfO solution. After exposing the original metallocycle to other anions (ReO₄⁻, BF₄⁻, and PF₆⁻), the TfO⁻ signal diminished significantly and the characteristic signals of PF₆⁻ (–68.85 and –71.37 ppm) and BF₄⁻ (–148.23 ppm) emerged, verifying the anion exchange processes. Based on the integration of the ¹⁹F NMR signals, the PF₆⁻/TfO⁻ and BF₄⁻/TfO⁻ ratios in the anion-exchanged metallocycle were ca. 5:1 and 15:1 respectively, i.e., the majority of the TfO⁻ anions were replaced by another counterion. While anion exchange took place rapidly in solution leading to an immediate precipitation of the metallocycle containing mostly the exchanged anions, the process was slow in the solid-state, as the ratio of two anions changed gradually with time before reaching the same ratio found during in-situ exchange after 3–4 days (Figure S2). These results suggested that the anion exchange took place in a single-crystal to single-crystal fashion as well as in solutions.

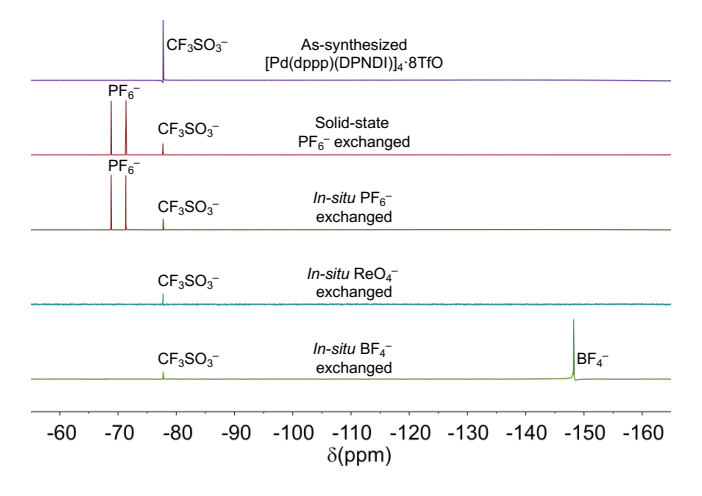


Figure 3. The ¹⁹F NMR (DMSO- d_6 , 282 mHz) spectra of [Pd(dppp)(DPNDI)]₄·8X (X⁻ = TfO⁻, ReO₄⁻, PF₆⁻, and BF₄⁻) metallocycles reveal anion exchange processes.

While the freshly prepared solutions of $[Pd(dppp)(DPNDI)]_4^{8+}$ metallocycle in DMSO- d_6 displayed the characteristic 1 H NMR signals of a single species, i.e., the tetrameric macrocycle, upon standing these NMR samples, colorless precipitates emerged over time, and the corresponding NMR spectra revealed the appearance of new species (Figure S1). Based on the integrals of 1 H NMR signals observed after several hours, the new species could be either a dumbbell-shaped 2:1 $[Pd(dppp)-DPNDI-Pd(dppp)]^{4+}$ complex or a $[Pd(dppp)(DPNDI)]_n^{2n+}$ coordination polymer. This observation was consistent with literature reports 18 of scrambling of pure Pd(II)-based metallosupramolecular squares into triangles and polymers in highly polar DMSO and DMF. Interestingly, upon gentle heating of these NMR samples, the precipitates redissolved and the characteristic spectra of original $[Pd(dppp)(DPNDI)]_4 \cdot 8X$ metallocycles reappeared.

Finally, irrespective of counterions, the cyclic voltammograms (Figure 4) of [Pd(dppp)(DPNDI)]₄·8X (*vs.* Ag/AgCl in respective 0.1 M Bu₄NX/DMF electrolyte solutions containing the same X⁻ anion) displayed two reversible one-electron reduction steps at ca. –0.33 and –0.81 V corresponding to DPNDI⁻ radical anion and DPNDI²⁻ dianion formation and a third reduction peak at –1.33 V associated with the Pd(II) reduction, indicating that the weak supramolecular interactions between the π-acidic DPNDI ligands and charge diffuse anions had little effect on the electronic properties of the metallocycle. The first electrochemical reduction of DPNDI, however, became slightly easier (~40 mV) upon the tetrameric macrocycle formation, as the coordination of two terminal pyridyl groups with Pd(II) corners made the NDI core even more electron deficient.

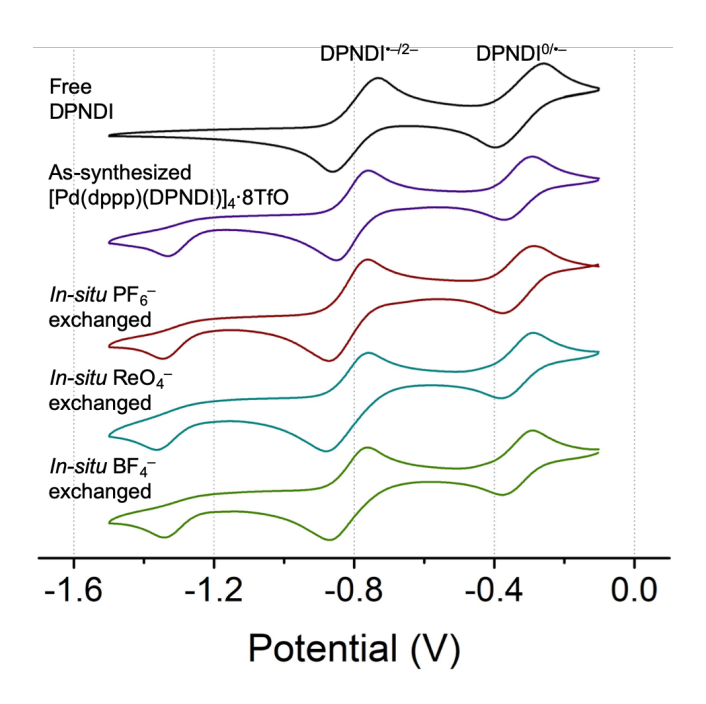


Figure 4. The cyclic voltammograms of free DPNDI ligand and $[Pd(dppp)(DPNDI)]_4 \cdot 8X$ ($X^- = TfO^-$, ReO_4^- , PF_6^- , and BF_4^-) metallocycles show little impact of weakly bound charge diffuse anions on the electronic property of DPNDI ligands.

In summary, we demonstrated the formation of a novel [Pd(dppp)(DPNDI)]₄⁸⁺ metallacycle and determined its crystal structure, which revealed various modes of anion/DPNDI interactions, providing valuable insights into its anion recognition and metathesis properties. The ¹H, ¹⁹F, and ³¹P NMR studies demonstrated that in noncoordinating solvents, the metallocycle underwent anion exchange in solutions as well as in a single-crystal to single-crystal fashion without experiencing structural changes, while polar coordinating solvents like DMSO led to gradual dissociation and scrambling, which could be reversed easily by a thermal treatment. Since the weak supramolecular interactions between charge diffuse anions

and π -acidic DPNDI ligands did not induce any significant spectroscopic and redox changes in the

metallocyclic receptor, the crystal structure proved to be an extremely valuable tool to determine its anion

recognition and exchange capabilities.

ASSOCIATED CONTENT

Supporting Information

The Supporting Information is available free of charge on the ACS Publications website at DOI: XXXXX.

Experimental details, additional data (PDF), and CIF file.

Accession Code

CCDC 1937603 contains crystallographic data, which can be obtained free of charge via

www.ccdc.cam.ac.uk/data request/cif, or by emailing data request@ccdc.cam.ac.uk, or by contacting The

Cambridge Crystallographic Data Centre, 12 Union Road, Cambridge CB2 1EZ, UK.

AUTHOR INFORMATION

*Corresponding Author

Email: souravs@clemson.edu

ORCID

Sourav Saha: 0000-0001-6610-4820

Note

The authors declare no competing financial interest.

ACKNOWLEDGEMENTS

This work was supported by the National Science Foundation (award no. CHE-1660329) and Clemson

University. We thank Drs. Colin McMillen, Ronald J. Clark, and Zhiyong Guo, for SXRD analysis and

structure elucidation.

REFERENCES AND NOTES

The single crystal X-Ray data of [Pd(dppp)(DPNDI)₄]·8OTf metallocycle with empirical formula

C₂₁₂H₁₅₂F₂₄N₁₆O₄₀P₈Pd₄S₈ and formula weight of 4949.33 was collected in a Bruker SMART APEX

II diffractometer at 103 K. The final unit cell dimensions were a = 26.460(4) Å, b = 15.550(3) Å, c

= 29.019(5) Å, $\alpha = 90^{\circ}$, $\beta = 105(2)^{\circ}$, $\gamma = 90(2)^{\circ}$. The structure was solved and refined using the

Bruker SHELXTL Software Package, in the monoclinic crystal system using the space group P2₁/c,

with Z = 2. The absorption coefficient was 0.526 mm^{-1} and a total of 41916 reflections were collected

9

- with 10386 [R(int)=0.1028] independent reflections. The final anisotropic full-matrix least-squares refinement on F2 with 646 variables converged at R1 = 11.40% for the observed data and wR2 = 34.90% for all data.
- (1) Chakrabarty, R.; Mukherjee, P. S.; Stang, P. J. Supramolecular Coordination: Self-Assembly of Finite Two- and Three-Dimensional Ensembles. *Chem. Rev.* **2011**, *111*, 6810–6918.
- (2) Würthner, F.; You, C.-C.; Saha-Möller, C. R. Metallosupramolecular Squares: From Structure to Function. *Chem. Soc. Rev.* **2004**, *33*, 133–146.
- (3) Cook, T. R.; Stang, P. J. Recent Developments in the Preparation and Chemistry of Metallacycles and Metallacages via Coordination. *Chem. Rev.* **2015**, *115*, 7001–7045.
- (4) Zarra, S.; Wood, D. M.; Roberts, D. A.; Nitschke, J. R. Molecular Containers in Complex Chemical Systems. *Chem. Soc. Rev.* **2015**, *44*, 419–432.
- (5) Pullen, S.; Clever, G. H. Mixed-Ligand Metal–Organic Frameworks and Heteroleptic Coordination Cages as Multifunctional Scaffolds—A Comparison. *Acc. Chem. Res.* **2018**, *51*, 3052–3064.
- (6) Chakraborty, S.; Newkome, G. R. Terpyridine-Based Metallosupramolecular Constructs: Tailored Monomers to Precise 2D-Motifs and 3D-Metallocages. *Chem. Soc. Rev.* **2018**, *47*, 3991–4016.
- (7) Cook, T. R.; Zheng, Y.-R.; Stang, P. J. Metal–Organic Frameworks and Self-Assembled Supramolecular Coordination Complexes: Comparing and Contrasting the Design, Synthesis, and Functionality of Metal–Organic Materials. *Chem. Rev.* **2013**, *113*, 734–777.
- (8) Furukawa, H.; Cordova, K. E.; O'Keeffe, M.; Yaghi, O. M. The Chemistry and Applications of Metal-Organic Frameworks. *Science*. **2013**, *34*, 2040–2042.
- (9) Ayme, J.-F.; Beves, J. E.; Leigh, D. A.; McBurney, R. T.; Rissanen, K.; Schultz, D. A Synthetic Molecular Pentafoil Knot. *Nat. Chem.* **2012**, *4*, 15–20.
- (10) Mitra, A.; Panda, D. K.; Corson, L. J.; Saha, S. Controllable Self-Assembly of Amphiphilic Macrocycles into Closed-Shell and Open-Shell Vesicles, Nanotubes, and Fibers. *Chem. Commun.* 2013, 49, 4601.
- (11) Vickers, M. S.; Beer, P. D. Anion Templated Assembly of Mechanically Interlocked Structures. *Chem. Soc. Rev.* **2007**, *36*, 211–225.
- (12) Stang, P. J.; Cao, D. H. Transition Metal Based Cationic Molecular Boxes. Self-Assembly of Macrocyclic Platinum(II) and Palladium(II) Tetranuclear Complexes. J. Am. Chem. Soc. 1994, 116, 4981–4982.

- (13) Fujita, M.; Yazaki, J.; Ogura, K. Preparation of a Macrocyclic Polynuclear Complex, [(En)Pd(4,4'-Bpy)]4(NO3)8 (En = Ethylenediamine, Bpy = Bipyridine), Which Recognizes an Organic Molecule in Aqueous Media. *J. Am. Chem. Soc.* **1990**, *112*, 5645–5647.
- (14) You, C. C.; Wüthner, F. Self-Assembly of Ferrocene-Functionalized Perylene Bisimide Bridging Ligands with Pt(II) Corner to Electrochemically Active Molecular Squares. *J. Am. Chem. Soc.* **2003**, 125, 9716–9725.
- (15) Goeb, S.; Bivaud, S.; Dron, P. I.; Balandier, J.-Y.; Chas, M.; Sallé, M. A BPTTF-Based Self-Assembled Electron-Donating Triangle Capable of C60 Binding. *Chem. Commun.* 2012, 48, 3106-3108.
- (16) Drain, C. M.; Lehn, J.-M. Self-Assembly of Square Multiporphyrin Arrays by Metal Ion Coordination. *J. Chem. Soc. Chem. Commun.* **1994**, *19*, 2313-2315.
- (17) Dinolfo, P. H.; Hupp, J. T. Supramolecular Coordination Chemistry and Functional Microporous Molecular Materials. *Chem. Mater.* **2001**, *13*, 3113–3125.
- (18) Krishnaswamy, S.; Prusty, S.; Chartrand, D.; Hanan, G. S.; Chand, D. K. Self-Assembled Molecular Squares as Supramolecular Tectons. *Cryst. Growth Des.* **2018**, *18*, 2016–2030.
- (19) Sautter, A.; Schmid, D. G.; Jung, G.; Würthner, F. A Triangle–Square Equilibrium of Metallosupramolecular Assemblies Based on Pd(II) and Pt(II) Corners and Diazadibenzoperylene Bridging Ligands. *J. Am. Chem. Soc.* **2001**, *123*, 5424–5430.
- (20) Weilandt, T.; Troff, R. W.; Saxell, H.; Rissanen, K.; Schalley, C. A. Metallo-Supramolecular Self-Assembly: The Case of Triangle-Square Equilibria. *Inorg. Chem.* **2008**, *47*, 7588–7598.
- (21) Stang, P. J.; Olenyuk, B. Self-Assembly, Symmetry, and Molecular Architecture: Coordination as the Motif in the Rational Design of Supramolecular Metallacyclic Polygons and Polyhedra. *Acc. Chem. Res.* **1997**, *30*, 502–518.
- (22) Schottel, B. L.; Chifotides, H. T.; Dunbar, K. R. Anion-π Interactions. *Chem. Soc. Rev.* **2008**, *37*, 68–83.
- (23) Mooibroek, T. J.; Gamez, P.; Reedijk, J. Lone Pair–π Interactions: A New Supramolecular Bond? *CrystEngComm* **2008**, *10*, 1501.
- (24) Müller, M.; Albrecht, M.; Sackmann, J.; Hoffmann, A.; Dierkes, F.; Valkonen, A.; Rissanen, K. CH-Anion versus Anion-π Interactions in the Crystal and in Solution of Pentafluorobenzyl Phosphonium Salts. *Dalt. Trans.* 2010, 39, 11329.

- (25) McDonald, K. P.; Hua, Y.; Lee, S.; Flood, A. H. Shape Persistence Delivers Lock-and-Key Chloride Binding in Triazolophanes, *Chem. Commun.* **2012**, *48*, 5065-5075
- (26) Chifotides, H. T.; Giles, I. D.; Dunbar, K. R. Supramolecular Architectures with π-Acidic 3,6-Bis(2-Pyridyl)-1,2,4,5-Tetrazine Cavities: Role of Anion-π Interactions in the Remarkable Stability of Fe(II) Metallacycles in Solution. *J. Am. Chem. Soc.* 2013, 135, 3039–3055.
- (27) Guha, S.; Saha, S. Fluoride Ion Sensing by an Anion–π Interaction. *J. Am. Chem. Soc.* **2010**, *132*, 17674–17677.
- (28) Guha, S.; Goodson, F. S.; Roy, S.; Corson, L. J.; Gravenmier, C. A.; Saha, S. Electronically Regulated Thermally and Light-Gated Electron Transfer from Anions to Naphthalenediimides. *J. Am. Chem. Soc.* **2011**, *133*, 15256–15259.
- (29) Guha, S.; Goodson, F. S.; Corson, L. J.; Saha, S. Boundaries of Anion/Naphthalenediimide Interactions: From Anion-π Interactions to Anion-Induced Charge-Transfer and Electron-Transfer Phenomena. J. Am. Chem. Soc. 2012, 134, 13679–13691.
- (30) Saha, S. Anion-Induced Electron Transfer. Acc. Chem. Res. 2018, 51, 2225–2236.
- (31) Ajayakumar, M. R.; Mukhopadhyay, P.; Yadav, S.; Ghosh, S. Single-Electron Transfer Driven Cyanide Sensing: A New Multimodal Approach. *Org. Lett.* **2010**, *12*, 2646–2649.
- (32) Ajayakumar, M. R.; Asthana, D.; Mukhopadhyay, P. Core-Modified Naphthalenediimides Generate Persistent Radical Anion and Cation: New Panchromatic NIR Probes. *Org. Lett.* **2012**, *14*, 4822–4825.
- Guha, S.; Goodson, F. S.; Clark, R. J.; Saha, S. Deciphering Anion–π-Acceptor Interactions and Detecting Fluoride Using a Naphthalenediimide-Based Pd(II) Coordination Polymer. CrystEngComm 2012, 14, 1213–1215.
- (34) Mitra, A.; Hubley, C. T.; Panda, D. K.; Clark, R. J.; Saha, S. Anion-directed assembly of non-interpenetrated square-grid metal-organic framework with nanoscale porosity. *Chem. Commun.* 2013, 49, 6629–6631
- (35). Mitra, A.; Clark, R. J.; Hubley, C. T.; Saha, S. Anion–π and CH····anion Interactions in Naphthalenediimide-Based Coordination Complexes. *Supramol. Chem.* **2014**, *26*, 296–301.
- (36) Zhang, W.-Y.; Han, Y.-F.; Weng, L.-H.; Jin, G.-X. Synthesis, Characterization, and Properties of Half-Sandwich Iridium/Rhodium-Based Metallarectangles. *Organometallics* **2014**, *33*, 3091–3095.

Table of Contents